Fitting freeform multi-parameter shapes to 3D data points – A case study

J.S.M. Vergeest, Y.Song

Delft University of Technology
Landbergstraat 15,
NL-2628 CE Delft
The Netherlands

j.s.m.vergeest@tudelft.nl

ABSTRACT

We present an approach of geometric fitting of freeform shapes to 3D data points, where the size of the fitting problem is relatively large. The shapes studied represent ship propeller blades of dimension up to 3m, with precision requirements of few mm. Moreover, the shapes are freeform and designed using a geometric model dependent on hundreds of numerical parameters. For the ship industry it is crucial to optimally deal with the shape parameters in order to judge whether or not a particular manufactured part fits within the tolerances. We have developed a method to evaluate the shapes numerically and we report on the approach we took. The sensitivity of a deviation objective function with respect to critical design parameters could be acquired. Also some procedures for automated optimization were explored.

Keywords

Propeller shapes, geometric design parameters, objective function, optimization, shape fitting

1. INTRODUCTION

Fitting of geometric shapes to predefined data points can be regarded as a special case of function fitting, where the function specifies a surface of dimensionality 2 in three-dimensional (3D) space. Shape fitting is a well developed technique applied in surface reconstruction for reverse engineering, or as part of a shape feature recognition process, for example [Chivate 1993, Bardinet 1998, Thompson 1999, Li 2000, Piegl 2001]. In most applications, the shape is modeled as function of shape parameters, for example when the shape is represented by B-spline functions (then the parameters are the control point coordinates), or as a form feature. In the latter case the parameters are called design parameters, since the parameters reflect a quantity which is relevant to the particular application or purpose of the shape.

Although designing new shapes starting from 3D range data is getting technically feasible [Vergeest 2003], the major purpose of 3D scanning and measurement is, historically, the verification of manufactured parts against design requirements. Reverse engineering of shape is mostly done in order to calculate and present spatial deviations between a physical object and a nominal geometric model of the object's surface.

In this paper we explore some ways to evaluate relatively complex shapes of ship propeller blades. These shapes have large dimensions (up to 3 meter each) and should meet high requirements of surface smoothness and geometric precision. The formal requirements of the shapes is evaluated according to quantities defined in ISO standard ISO 484 of manufacturing tolerances [ISO 1981]. To evaluate the shape of a propeller blade against the standard it is sufficient, in industry, to measure a relatively small number (about 100) of surface points. It is obvious that practicing the right methodology for shape evaluation is critical, since the rejection of a manufactured propeller would be extremely costly. In section 2 we describe the nominal model of the shape and the definition of the design parameters, and the general process of shape evaluation. In section 3 we investigate the sensitivity of the geometric deviation function on critical shape parameters. In section 4 we propose a semi-automatic method to determine whether or not a shape conforms to the ISO requirements. An outlook to application of the method to larger number of parameters is given in section 5.

2. DESIGN AND MEASUREMENT OF THE GEOMETRIC SHAPES

The purpose of a propeller is to deliver propulsion to a ship by pressing water backwards with its rotating blades. The shape of a blade is designed to move water particles into the direction of its axis of rotation. The distance that a water particle would theoretically be moved during one full revolution of the propeller is called the pitch of the blade. Once the requirements of the propeller are determined by the customer, the designer creates the shapes. The actual production is achieved by filling molds with a copper alloy. The inner shape of the molds is not exactly equal to the shape of the blade, since there should be compensation for shrinkage of the metal after cooling down. In this paper we will only consider the nominal model of the shape, as designed, and the shape of a physical propeller blade after its manufacturing (Figure 1).

Figure 1. Example of a propeller blade. The marks on the surface indicate the locations of the verification measurements.

The model of the shape B is constructed from m profile curves G'_1, ..., G'_m, where G'_i defines the intersection of B with a cylinder of radius r_i with axis equal to the rotation axis of the propeller. However, G'_i is specified by the designer as the development G_i of the closed curve onto the xy-plane. Profile G_i is specified by n points g_{ij} with coordinates (x_{ij}, y_{ij}), i=1, ... ,m, j=1, ..., n. Here we assume that n is the same for all profiles. To each profile G_i the following quantities are assigned, which will determine the mapping of G_i into $\mathbb{R}^3$:

- r_i is the radius of the cylinder onto which the points g_{ij}, j=1,...,n will be placed.
- ϕ_i is the pitch angle designed for the profile. The pitch angle determines the pitch distance (defined below). A pitch angle can be designed (implemented) by rotating the profile in the xy-plane by that angle.
- p_i is the pitch distance, defined as the theoretical amount of shift due to a screw revolution of 360 degrees, or $p_i = 2\pi r_i \,\mathrm{tg}\, \phi_i$. and hence ϕ_i = atan $p_i/2\pi r_i$.
- σ_i is the skew distance designed for the profile. It is implemented by a shift of the profile in the surface of the cylinder in a direction perpendicular to its axis.
- ρ_i is the rake distance designed for the profile. It is implemented by a shift of the profile in the surface of the cylinder into a direction parallel to its axis.

Examples of a profile curve is shown in figure 2.

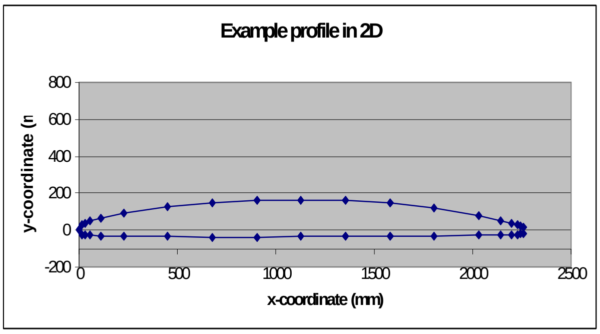

Figure 2. One of the profiles G_i of an example blade design.

The profiles G_i are mapped into space by applying the transformation T_i to each of its points g_{ij} as follows:

$$g'_{ij} = T_i\,(g_{ij}) = T_i(x_{ij}, y_{ij}), \qquad (1)$$

such that

$$g'_{ij} = \begin{pmatrix} x'_{ij} \\ y'_{ij} \\ z'_{ij} \end{pmatrix} = \begin{pmatrix} r_i \sin(f_{ij}) \\ r_i \cos(f_{ij}) \\ \rho_i + (x_{ij} - \sigma_i)\sin(\phi_i) - y_{ij}\cos(\phi_i) \end{pmatrix}$$

and

$$f_{ij} = (-y_{ij}\sin(\phi_i) - (x_{ij} - \sigma_i)\cos(\phi_i)) / r_i\,.$$

From the points g'_{ij} the mapped profiles G'_i can be derived for i=1,...,m and from these the nominal blade design B. Figure 3 shows the points g'_{ij} of an example blade design with m=25.

Equation (1) implies the coordinate system convention used, which differs from the one depicted in [ISO 1999].

From (1) we see that in 3D points g'_{ij} are located on cylinders with axes in the z-axis of the coordinate system.

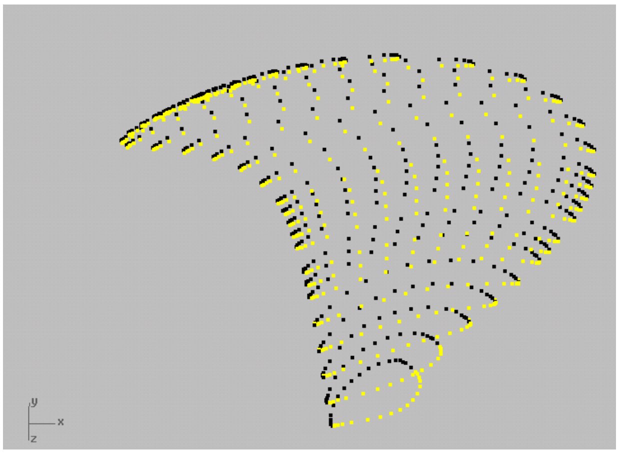

Figure 3. Profile points positioned in 3D space using equation (1).

In the simplest case, if rake, skew and pitch are vanishing, a profile point in the origin of the 2D plane is placed in 3D at the intersection of the *y*-axis with the cylinder. Points with positive *x*-values in the 2D plane will be positioned with negative *x*-coordinates in 3D, since f_{ij} is getting negative. Points with positive *y* in 2D will have lower *z*-coordinates in 3D. Now, if the pitch angle (or pitch distance) is set to a positive value, points in the profile having large *x*-values in the 2D plane move up into positive *z*-direction in 3D. In other words, due to increasing pitch the profile is rotated in 3D about the *y*-axis in the positive sense, *i.e.* counterclockwise, and thus influences the shape of the propeller. If the propeller is operated and be rotated clockwise about the *z*-axis, the profile would then be rotated clockwise about the *z*-axis and the water be pressed into the positive *z*-direction and thus the ship be propelled into the negative *z*-direction. Then the water is pushed by the pressure side, as it should for forward propulsion of the ship. The shape of the blade resulting from equation (1), see Fig. 4, should be interpreted in 3D relative to the ship as follows. The forward direction of the ship is in the negative *z*-direction, the *y*-direction is vertically upward and the *x*-direction is horizontal to the right as seen from an observer on the ship looking forward. The blade is orientated such that the line from axis of rotation toward the tip of the blade is roughly into the positive *y*-direction. As seen from behind the ship the blade is pointing upward and its pressure surface is visible. Due to forward operation the tip of the blade has a speed into the positive x-direction. The profile point located nearest to the origin of the 2D plane (as in Fig. 2) will in 3D have the largest x-value and will move into the positive *x*-direction and therefore is a point on the so-called leading edge of the blade. The concave part of the profile (the lower part in Figure 2) is facing the positive z-direction in 3D and is hence in the pressure surface. A drop of water near the pressure surface of the blade will observe the surface moving toward it and receive a momentum into the positive *z*-direction.

If the pitch would increase then the shape in Fig. 5 would be further twisted about *y*. If the rake of a particular profile gets positive, then in 3D the profile shifts into the positive *z*-direction, according to equation (1). When its skew increases, the profile moves into the positive *x*-direction in 3D. Obviously, rake and skew have a smaller effect on the performance of the screw than has the pitch.

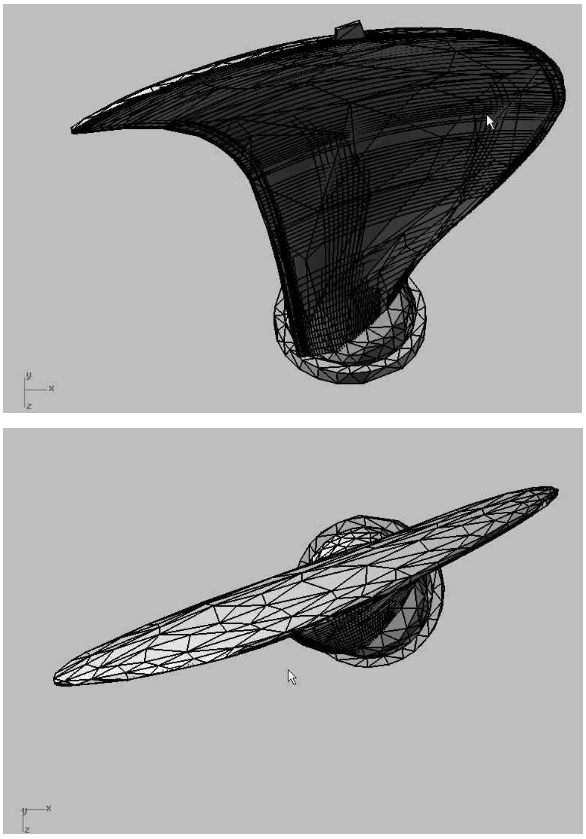

Figure 4. Shape of *B* in 3D space after applying equation (1) to the profile points.

The model depicted in Fig. 4 includes the foot of the blade, which was not represented by the profile points. We show this picture to provide a clear impression of the positioning of the blade relative to the propeller and the ship. However, from this point on, we will refer to a simpler shape design directly obtained from the profile points, see Fig. 5. This shape is used for the computation of distances between measured points on a surface and the designed surface later. The shape consists of two B-spline surfaces, one representing ∂B_p (the pressure surface as designed) and the other ∂B_s (the suction surface) . The pressure surface in Fig. 5 was obtained from the designed profile points g'_{ij} as follows. The profile points form two networks of $m \times n$ = 25×19 points

 ISBN 978-80-86943-94-7

each, one for the pressure surface, one for the suction surface. Using a tensor-product B-spline approximation method [VNI 2006] we determined the B-spline surface of polynomial degree 3 in both directions, having 15 control points in each direction approximating the profile point network of the pressure surface in a least-squares sense. The suction surface ∂B_s was obtained similarly.

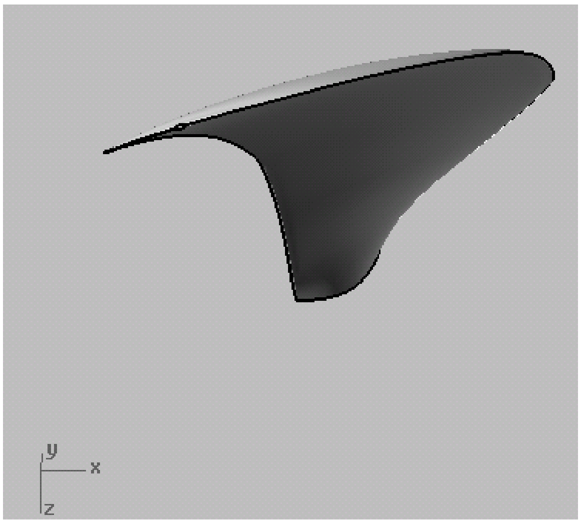

Figure 5. Shape of *B* consisting of two B-spline surfaces fitted to the profile points in 3D.

Once a blade *B* has been manufactured it is inspected as to verify whether its shape fits within the tolerances supplied by the customer. The current procedure at the Wärtsilä company includes the digitization of the shape of physical part *B*. Typically, about 100 data points are acquired of each of the two surfaces, ∂B_p and ∂B_s. Let us denote these two point sets by p_i and s_i, where p_i, $s_i \in \mathbb{R}^3$ and *i* is an index from 1 to the number of points in the set. The locations of the measured points p_i and s_i relative to the designed shapes are shown in Fig. 6 for the example model. Suppose that the data points p_i are all in front of the designed surface ∂B_p when viewed from an angle as in the upper picture of Fig. 6. Then, in case the deviation would exceed a tolerance it could be resolved by machining or polishing material away from the pressure side of *B*. However, when the data point would be behind the designed surface, there is a risk that *B* is too thin, and there were no correction possible by machining. It is therefore the general policy to produce *B* for which $p_{iz} < p'_{iz}$ for all *i*, where p_{iz} is the *z*-coordinate of p_i and p'_{iz} is the *z*-coordinate of p'_i , the point in ∂B_p closest to p_i. Similarly, $s_{iz} > s'_{iz}$ for all s_i and s'_i is the point in ∂B_s nearest to s_i. In the particular example shown in Fig. 6 the *z*-residuals have all have that property.

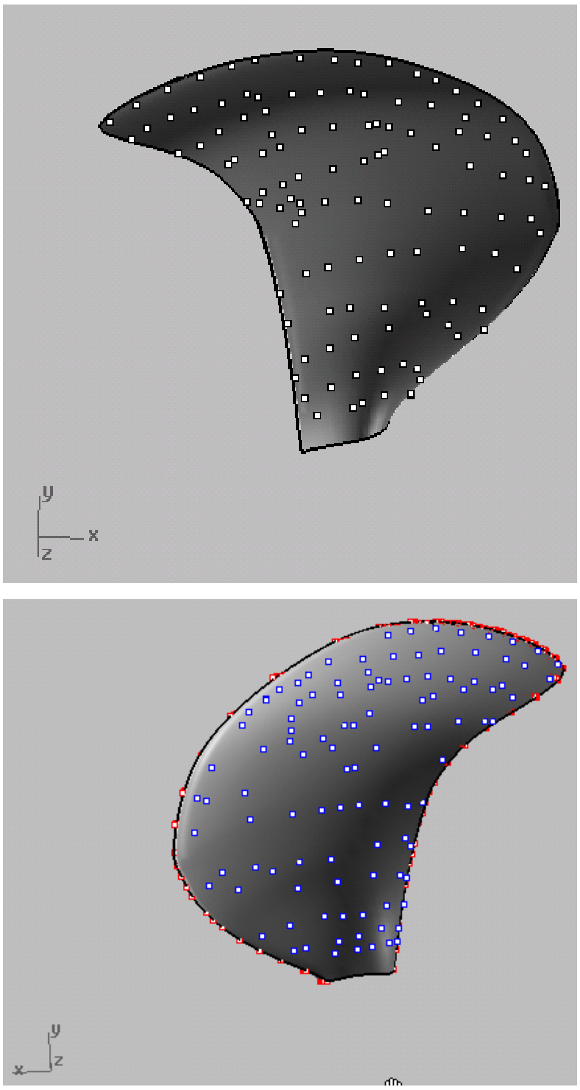

Figure 6. B-spline surface representing the pressure surface and points measured on it (top); same picture of the suction surface (bottom).

In Fig. 7 the distribution *z*-differences D_z, calculated as $p_{iz} - p'_{iz}$ and $s_{iz} - s'_{iz}$,have been plotted. The D_z against the radius of the data points, *i.e.* their distance from the *z*-axis, are shown in Figure 8. The data points appear in a vertical linear pattern, due to the fact that the surface was measured at about 5 positions on a profile of a particular cylindrical radius *r*.

3. SENSITIVITY ANALYSIS OF SHAPE PARAMETERS

Instead of correcting physical part *B* itself we can (at least theoretically) also modify the design *B* as to fulfill the measurement conditions $p_{iz} - p'_{iz} > 0$ and $s_{iz} - s'_{iz}. < 0$ (if necessary) and/or to decrease the mean error of the physical part against the modified nominal design model.

 ISBN 978-80-86943-94-7

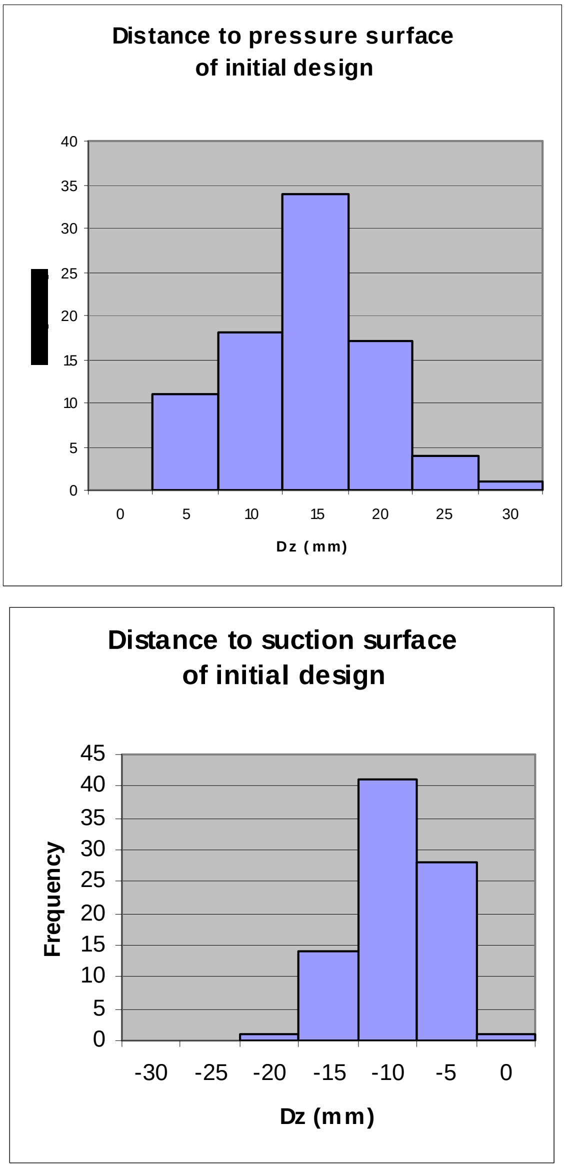

Figure 7. Distribution of signed *Z*-residuals of the measured data points to the nominal surface of the blade.

In doing so, the negotiation between customer and supplier is made in terms of design parameters, rather than in terms of spatial deviations of measured points from the nominal shape. We wish to gain understanding of the effect on the shape due to modification of shape parameters. The parameters which are the least critical to the performance of a propeller are the rake parameters ρ_i. Suppose that the design fulfills all requirements is still not optimal. Then modification of rake could improve the shape while remaining meeting the requirements. This offers an opportunity to optimize a manufacturing condition

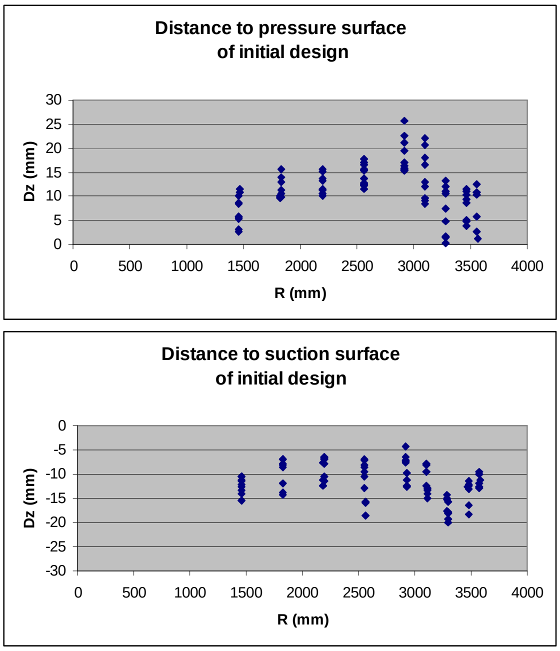

Figure 8. *Z*-residuals of the measured data points versus their radius.

From equation (1) it follows that if the rake ρ_i of some profile(s) G_i is increased by a positive amount a then the values p'_{iz} and s'_{iz} will increase by an amount between 0 and a, depending on the location of the surface point relative to the changed profiles. In terms of the two plots in Fig. 8 it means that points in both plots will move down when a is increased and will move up when decreased From Fig. 8 it can be reasoned that at r near 3500mm the rake should not be increased since it would make some of the D_{zi} for the suction side negative and thus bring some data points inside the blade's volume. A decrease of the rake would be admitted. The largest deviation between data points and suction surface occurs at $r \approx$ 3000mm, so an increase of rake in that region might improve the shape fit in a least-squares sense.

We performed a numerical sampling of rake values ρ'_i around the design values ρ_i by setting:

$$\rho'_i = \rho_i + A_1 \quad \text{for} \quad 1 \leq i < 5$$
$$\rho'_i = \rho_i + A_2 \quad \text{for} \quad 5 \leq i < 9 \qquad (2)$$
$$\rho'_i = \rho_i + A_1 \quad \text{for} \quad 9 \leq i < 13,$$

where we used step sizes of 5mm for A_1, A_2 and A_3. The index i=1 corresponds to the data points on the profile with largest radius, r_1 = 3650mm, and the highest, $i = m = 25$, for this particular blade design, the radius is r_{25} = 730mm. The A-parameters influence the rake values and thus the position of the design points g'_{ij} as follows. A_1 affects points in the region of approximately 3600mm < r < 3650mm, A_2 in the region 3100mm < r < 3600 and A_3 in the region

Table 1. Deviation of data points from the shape for three configurations.

Measure	Initial design	$A_{1,2,3}$ = (-20, -5, +5)	Free ρ_0 ... ρ_{11}
Dist. sq. P (mm^2)	15609.3	13644.7	16059.2
Dist. sq. z P (mm^2)	13103.8	10991.3	13565.8
Av. dist. P. (mm)	12.5	11.9	12.9
Max. dist. P (mm)	26.9	21.1	27.2
Dist. sq. S (mm^2)	18442.2	19684.8	15885.3
Dist. sq. z S (mm^2)	12391.2	13897.0	11223.5
Av. dist. S (mm)	13.8	14.5	12.7
Max. dist. S (mm)	27.4	27.0	25.9
Dist. sq. P and S (mm^2)	34051.4	33329.5	31944.5

2370mm < r < 3100mm. The best fit by sampling was obtained for A_1 = –20mm, A_2 = –5mm and A_3 = +5mm. We also performed a shape fit with ρ_0 ... ρ_{11} as independent free parameters. The results of the analysis are shown in the second data column of Table 1.

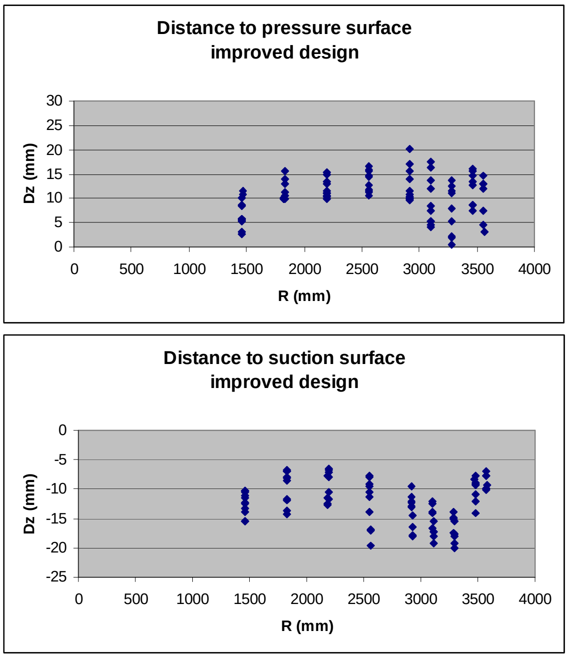

Figure 9. Z-residuals of improved shape design, for optimal A_1, A_2 and A_3.

The sums of the distances squared from the measurements of the pressure surface (P) and suction surface (S) are presented, as well as the average and maximum distances.

We performed a 12-parameter fit where the objective function was the sum of the two sums of distances squared, displayed in the lower row of Table 1. The result from the 12-parameter fit, listed in the rightmost column of Table 1, is not realistic, since the rake values deviate strongly (between 10 and 1000mm) from the original design, leading to a distorted shape of the blade (not shown). So, although the fitting criterion is well satisfied, the shape would be unacceptable. The method of stepwise varying sets of 3 adjacent rake values, as in equation (2) provides a more reliable result. The individual data points for this configurations are shown in Figure 9, and can be compared to Figure 8. One improvement of the design in Figure 9 is the reduction of the error at the pressure surface around r = 2900mm. It goes at the cost of a slightly larger sum of squared distances at the suction surface, but the total error, of both surfaces together reduces from 34051.4mm^2 to 33329.5mm^2.

We study the effect of changing rake more closely by varying A_3 around its best value A_3 = 5mm found during the rough stepwise sampling. The quantities defined for Table 1 are plotted as a function of A_3 in Figure 10.

 ISBN 978-80-86943-94-7

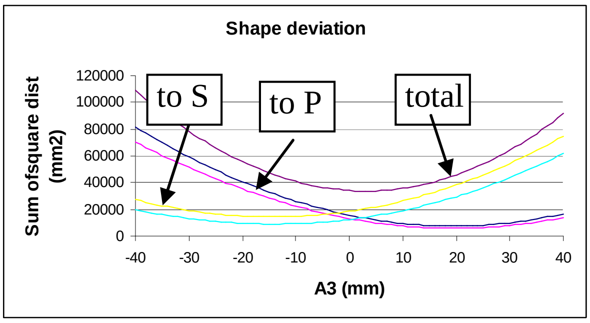

Figure 10. Deviation of shape from data points a function of deviation of rake with indices 7 to 11.

The sum of distances squared of the data points measured on the pressure surface (labeled “to P” in Figure 10) is minimal for $A_3 \approx 19$mm, compared to $A_3 \approx -14$mm for the suction side. The total sun of distances squared in the *z*-direction are shown as well. The total sum reaches its minimum at $A_3 \approx 3$mm.

4. POSSIBLE FITTING STRATEGY

The minimal total sum (as used for Figure 10) is a criterion for goodness of shape, since it implies that material should be removed from both sides of the physical part in order to achieve zero-error. However, care should be taken that the modified shape design never touches or encloses data points.

As mentioned, leaving each rake value as a free parameter in a fit does not work properly. The main reason for this is the instability of shape generation from the design points g'_{ij}. This problem does not occur during the regular design process, where the overall smoothness of the shape is controlled. For the purpose of the numerical experiments, however, we used a simpler, faster shape generation method as to keep the objective function efficient. In this simplified method it can occur that the shape becomes wavy when subsequent rakes are changed very unevenly. To avoid those fluctuations, we varied the rake values in sets, as in equation (2). The result of such a fit is shown in Table 2. Indeed the total sum of squared distances is reduced compared to the estimated values in the middle data column of Table 1, however at the cost of a larger distance at the pressure side of the blade.

The fitting result in Table 2 was obtained by setting the starting values for A_1, A_2 and A_3 to -20, -5 and 5. When choosing different starting values, the fit typically appear to be worse.

Table 2. Fit of shape to data points with free parameters A_1, A_2 and A_3.

Measure	$A_{1,2,3}$= **(–20.0, –5.2, 3.5)**
Dist. sq. P (mm^2)	15228.2
Dist. sq. *z* P (mm^2)	12345.6
Av. dist. P. (mm)	12.7
Max. dist. P (mm)	23.0
Dist. sq. S (mm^2)	17640.9
Dist. sq. *z* S (mm^2)	12381.9
Av. dist. S (mm)	13.7
Max. dist. S (mm)	26.2
Dist. sq. P and S (mm^2)	32869.1

The fitting strategy could be composed as follows:

1. Import the data points from measurements of the pressure side and the suction side of the propeller blade(s).
2. Calculate the deviation of the data points from the nominal design of the blade surface.
3. If any of the data points is contained in the volume of the nominal model or if any data point is too far off from the nominal design, issue a message.
4. Starting form the nominal design parameters, minimize the total of the sums of squared distances of data points to the shape, where a subset of the shape parameters are free in the fitting procedure.
5. Perform some sampling of the free parameters and conduct the action as described in step 4. If any shape is found better fitting the data points, then save these parameter values.
6. Verify whether this shape is conform the specifications of the customer. If not reiterate step 5.
7. Use the resulting shape to generate a milling or grinding process to achieve a physical part matching a design.

5. DISCUSSION

We have shown for a particular case that instead of the shape of the nominal design, an improved shape can be found to control the final machining process of the physical part. The new shape can provide a better balanced machining result because the shape is "positioned" halfway the data points of the pressure surface and those of the suction surface. Then the amounts of material to be removed from the two sides are approximately equal, making the machining process more efficient.

Using the simplified surface construction method, the objective function of the fitting procedure is sufficiently efficient as to generate new shape proposal in about 100s or less. However, as mentioned, there is a small deviation between the shape constructed using the company's high-end CAD system and the shape we obtained by a straightforward least-squares cubic B-spline surface fitting against the design points g'_{ij} of equation (1). In this B-spline fit, there are multiple options for the B-spline knot vector and the polynomial degree of the B-spline functions [VNI 2006]. There is also an issue in the computation of the distance between a data point to the B-spline surface. Finding the point in the B-spline surface closest to a given data points depends on a Quasi-Newton fit with the *u*- and *v*- parameters of the B-spline surface as free parameters. In some cases this fit produces a wrong local minimum, and thus fails to find the closest point. We could solve this issue by choosing 16 points evenly dispersed in the *uw*-space, and performing the distance computation with each of these 16 points as starting values.

As mentioned, the fitting procedure for shape against data points can produce unreliable results. The Quasi-Newton algorithm typically outputs a local optimum near the starting values supplied. Even if the number of parameters is kept as low as three (as we did with the A_i fits), finding the global optimum requires presampling of the parameter space. Whereas this proved feasible for three parameters, it would become impractical for 10 or more parameters. A more sophisticated search algorithm, dedicated to the specific geometric characteristics of propeller blades should be developed. It is unlikely that such an algorithm would work on the data consisting of as few as about a hundred points on each side of the blade. A medium dense point set, of about 5000 points on each surface side is required.

As mentioned, the pitch is a more critical parameter than the skew and rake are. Still, very small changes to the pitch of the nominal design model based on measurements of the produced part, could improve the final machining process as we showed for changes of rake, that is better balanced removal of material. However, if the measurements would reveal that the pitch values are not as designed (and maybe even exceed the tolerances) then it can be attempted to create a new design model with improved pitch values, but still contained within the volume of the manufactured part.

6. REFERENCES

[ISO 1981] "International Standard ISO 484/1, Shipbuilding – Ship screw propellers – Manufacturing tolerances". ISO, Geneva, 1981.

[ISO 1999], Propulsion plants for ships – Terms and definitions – Part 1: Geometry of propellers. Draft International Standard ISO/DIS 3715-1, ISO, Geneva 1999.

[Li 2000] Li, C. L., and Hui, K. C., 2000, "Feature Recognition by Template Matching," Comput. Graph., **24,** pp. 569–583.

[Chivate 1993] Chivate, P. N., and Jablokow, A. G., 1993, "Solid-Model Generation From Measured Point Data," Comput.-Aided Des., **25**, pp. 587–600.

[Bardinet 1998] Bardinet, E., and Cohen, L. D., 1998, "A Parametric Deformable Model to Fit Unstructured 3D Data," Comput. Vis. Image Underst., **71**, pp. 39–54.

[Piegl 2001] Piegl, L. A., and Tiller, W., 2001, "Parametrization For Surface Fitting in Reverse Engineering," Comput.-Aided Des., **33**s8d, pp.593-603.

[Vergeest 2003] Vergeest, J. S. M., Spanjaard, S. and Song, Y., 2003, "Directed Mean Hausdorff Distance of Parameterized Freeform Shapes in 3D: A Case Study," Visual Comput., **19**, pp. 480–491.

[Thompson 1999] W.B. Thompson, J.C. Owen, H. James de St. Germain, S.R. Stark and T.C. Henderson, "Feature-based reverse engineering of mechanical parts", IEEE Tran. Robotics and Automation, Vol. 15, No 1, 1999, pp. 57-66.

[VNI 2006] Visual Numerics, IMSL C Numerical Library Version 6.0, Visual Numerics, Houston, 2006.